

# Contrast Interferometry using Bose-Einstein Condensates to Measure $h/m$ and

S. Gupta, K. Dieckmann, Z. Hadzibabic and D. E. Pritchard

Department of Physics, MIT-Harvard Center for Ultracold Atoms, and Research Laboratory of Electronics,  
MIT, Cambridge, MA 02139  
(November 10, 2021)

The kinetic energy of an atom recoiling due to absorption of a photon was measured as a frequency using an interferometric technique called "contrast interferometry". Optical standing wave pulses were used as atom-optical elements to create a symmetric three-path interferometer with a Bose-Einstein condensate. The recoil phase accumulated in different paths was measured using a single-shot detection technique. The scheme allows for additional photon recoils within the interferometer and its symmetry suppresses several random and systematic errors including those from vibrations and ac Stark shifts. We have measured the photon recoil frequency of sodium to 7 ppm precision, using a simple realization of this scheme. Plausible extensions should yield a sufficient precision to bring within reach a ppb-level determination of  $h/m$  and the fine structure constant.

PACS numbers: 39.20.+q, 3.75.Dg, 6.20.Jr, 3.75.Fi

Comparison of accurate measurements of the fine structure constant in different subfields of physics – e.g. atomic physics, QED and condensed matter physics – is one of the few checks for global errors across these different subfields. The  $(g/2)$  measurement for the electron and positron together with QED calculations, provides a 4 ppb [1,2] measurement of  $\alpha$ . This has stood as the best measurement of the fine structure constant since 1987. The second most accurate published value of  $\alpha$ , at 24 ppb comes from condensed matter experiments [3]. This is worse by a factor of six, limiting the scientific value of cross-field comparisons. A new and more robust route based on atomic physics measurements has emerged in the last decade [4]:

$$\alpha^2 = \frac{e^2}{\hbar c}^2 = \frac{2R_1}{c} \frac{\hbar}{m_e} = \frac{2R_1}{c} \frac{M}{M_e} \frac{\hbar}{m} : \quad (1)$$

The Rydberg constant  $R_1$  is known to 0.008 ppb [5,6] and the electron mass  $M_e$  to 0.7 ppb [7].  $M$  and  $m$  are the mass of some test particle in atomic and SI units respectively. Eq.1 offers the possibility of a ppb level measurement of  $\alpha$  if  $M$  and  $h/m$  can be determined accurately.

$h/m$  can be measured by comparing the deBroglie wavelength and velocity of a particle, as demonstrated by Kugler, whose measurement using neutrons has yielded a value for  $h/m_n$  accurate at 73 ppb [8]. For an atom,  $h/m$  can be extracted from a measurement of the photon recoil frequency

$$\omega_{\text{rec}} = \frac{1}{2m} \hbar k^2 ; \quad (2)$$

where  $k$  is the wavevector of the photon absorbed by the atom. Recent experiments allow Eqs.1,2 to be applied to cesium.  $M_{\text{Cs}}$  is known to 0.17 ppb [9] and  $k_{\text{Cs}}$  to 0.12 ppb [10].  $\omega_{\text{rec,Cs}}$  has been measured at Stanford using an atom interferometer based on laser-cooled atoms [12-14] to 10 ppb [11]. Similar experiments are also possible

with alkali atoms like sodium and rubidium where  $M$  has been measured [9] and  $k$  is accurately accessible [10].

In this Letter, we demonstrate a new atom interferometer scheme which shows promise for a high precision measurement of  $\omega_{\text{rec}}$ . Our symmetric three-path configuration encodes the photon recoil phase in the contrast of the interference fringes, rather than in their phase. Because it is insensitive to the fringe phase, the method is not sensitive to vibrations, accelerations or rotations. The symmetry also suppresses errors from magnetic field gradients and our use of only one internal state suppresses errors arising from differences in the ac Stark shifts between different internal states. A crucial aspect of this new interferometer is the use of atomic samples with sub-recoil momentum distribution. We use a Bose-Einstein condensate (BEC) as a bright atom source. This allows the contrast oscillations to persist for many cycles, permitting precise determination of the recoil phase in a single "shot" and also allows for extra photon recoils to be added within the interferometer, increasing the recoil phase shift quadratically.

The Stanford scheme to measure  $\omega_{\text{rec}}$  uses different internal states to separately address different interferometer paths, allowing a linear increase of measurement precision by additional photon recoils. However, vibrations and ac Stark shifts have been of great concern in this scheme [13]. An alternative interferometer to measure the photon recoil using laser cooled atoms in a single internal state was demonstrated using rubidium atoms [15]. Like ours, this scheme also incorporates a symmetric arrangement and operates by measuring contrast. This interferometer should also suppress vibration noise and systematics arising from ac Stark shifts between different internal states. However, different paths cannot be individually addressed in this scheme, making it difficult to extend to competitive precision. Our interferometer extends these previous schemes and combines their advantages. The precision of the Stanford scheme increases linearly with additional recoils. Quadratic scal-

ing schemes have been proposed [16] and demonstrated in a multi-path interferometer based on dark states [17]. However, the number of additional recoils in this scheme, is limited by the internal atomic structure.

Our scheme is based on the asymmetric interferometer of Fig. 1 (a). At time  $t = 0$  a BEC is split coherently into two momentum components,  $|j\hbar k\rangle$  and  $|j\hbar k\rangle$ , by a first order Bragg  $\pi$ -pulse [18]. These are shown as paths 1 and 2 in the figure. At time  $t = T$ , a second order Bragg  $\pi$ -pulse reverses the direction of path 1, while leaving path 2 unaffected. Around  $t = 2T$ , a moving matter wave grating, with spatial periodicity  $\lambda = 2$  (wavevector  $2k = \frac{2\pi}{\lambda}$ ), is formed due to the overlap and interference of the two paths. The phase of this grating at  $2T$  is determined by the relative phase  $\phi_1 - \phi_2 = 8\pi \frac{m}{h} T$ , accumulated between paths 1 and 2 due to the difference in their kinetic energies. A measurement of this phase for different values of  $T$  will then determine  $\frac{m}{h}$ . If the momentum of path 1 is increased  $N$  times by additional photon recoils, the corresponding grating phase will be  $\phi_1 - \phi_2 = N^2 8\pi \frac{m}{h} T$ , leading to an  $N^2$ -fold improvement in the measurement precision. The fringes of all atoms will be in phase at  $2T$ , forming a high-contrast matter wave grating. This dephases in a time  $\frac{1}{k \cdot v}$ , the coherence time, where  $v$  is the atomic velocity spread.

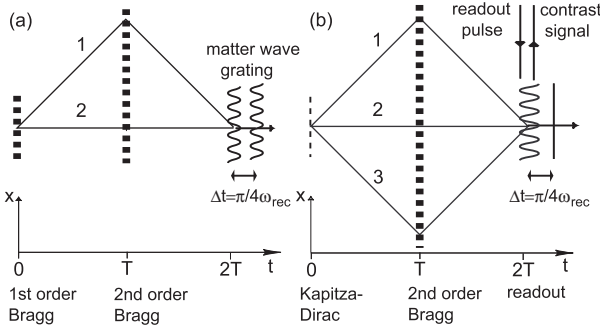


FIG. 1. Space-time representation of the contrast interferometer. (a) shows a simple 2-path interferometer sensitive to the photon recoil phase. The  $2k$  matter wave grating is shown at  $2T$  and at  $2T + \lambda = 4\lambda_{\text{rec}}$ . The extension to the 3-path geometry is shown in (b). The overall  $2k$  grating has large contrast at  $2T$  and zero contrast at  $2T + \lambda = 4\lambda_{\text{rec}}$ .

Extension of this interferometer to a symmetric three-path arrangement is shown in Fig. 1 (b). Three momentum states (paths 1, 2 and 3) are generated by replacing the first Bragg pulse with a short Kapitza-Dirac pulse [18]. At  $t = 2T$ , there are now two matter wave gratings with period  $\lambda = 2$ , one from paths 1 and 2 and one from paths 2 and 3. These move in opposite directions at a relative speed  $4\hbar k/m$ . If the maxima of the two gratings line up to produce large contrast at time  $t$ , the maxima of one will line up with the minima of the other at  $t + \lambda = 4\lambda_{\text{rec}}$ , to produce zero contrast. This results in an oscillatory growth and decay of the contrast of the overall pattern with time. The recoil induced phase can

be determined from this temporally oscillating contrast.

The time evolution of this contrast can be monitored by continuously reflecting a weak probe beam from the grating (the additional grating formed by paths 1 and 3 has period  $\lambda = 4$ , which does not reflect the probe beam). The reflected signal can be written as

$$S(T; t) = C(T; t) \sin^2 \left( \frac{\phi_1(t) + \phi_3(t)}{2} \right) \quad (2)$$

$$= C(T; t) \sin^2 (8\pi \frac{m}{h} T + 4\pi \frac{m}{h} (t - 2T)); \quad (3)$$

where  $C(T; t)$  is an envelope function whose width is the grating coherence time,  $\frac{1}{k \cdot v}$ . This motivated our use of a BEC atom source. This allowed many contrast oscillations in a single shot. Using the phase of the reflection at  $t = 2T$ ,  $\phi_1(T) = 8\pi \frac{m}{h} T$ ,  $\frac{m}{h}$  can be determined by varying  $T$ . Vibrational phase shifts and the effect of magnetic bias fields gradients cancel in the evaluation of  $\frac{\phi_1(t) + \phi_3(t)}{2}$ , due to the symmetry of our scheme.

In this experiment, we realize the scheme of Fig. 1 (b) and measure  $\frac{m}{h}$  to 7 ppm precision. We also demonstrate the insensitivity of the contrast signal to vibrations and the  $N^2$  scaling of the recoil phase.

We used sodium BEC's containing a few million atoms in the  $F = 1; m_F = -1$  state as our atom source. The light pulses were applied 15 ms after releasing the BEC from a weak magnetic trap. This lowered the peak density to about  $10^{13} \text{ cm}^{-3}$ , thus preventing super-radiance effects [19] and reducing frequency shifts from mean field interactions. Two horizontal counterpropagating (to 1 mrad) laser beams were used for the diffraction gratings. The light for the gratings was red-detuned by 1.8 GHz from the sodium  $D_2$  line. Rapid switching ( $< 100 \text{ ns}$ ) and intensity control of the light pulses was done by an acousto-optic modulator (AOM) common to the two beams. The phase and frequency of each beam were controlled by two additional AOMs, driven by two phase-locked frequency synthesizers.

The interferometer pulse sequence was started with a 1  $\mu\text{s}$ , square Kapitza-Dirac pulse, centered at  $t = 0$ . We adjusted the beam intensity, to put 25% of the condensate in each of the  $j \pm 2\hbar k$  diffracted orders. This choice yielded the best final contrast signal. The second order Bragg pulse was centered at  $t = T$  and was close to Gaussian shaped with a width of 7.6  $\mu\text{s}$ . The intensity was chosen to effect a  $\pi$ -pulse between the  $j \pm 2\hbar k$  states. The smooth pulse shape reduced the off-resonant population of undesired momentum states, yielding a transfer efficiency of  $> 90\%$ . The third pulse, used for reading out the contrast signal, was centered at  $t = 2T$  and was typically 50  $\mu\text{s}$  long. One of the Bragg beams was used as the readout beam while the other was blocked.

The light reflected from the atoms was separated from the readout beam path using a beam splitter and directed by an imaging lens onto a photomultiplier. A typical interferometer signal is shown in Fig. 2. We observed the

expected contrast oscillations at frequency  $8!_{\text{rec}}$ , corresponding to a 5 s period for sodium. We obtained the recoil phase ( $T$ ) from the contrast signal by fitting to a sinusoidal function as in Eq.3.

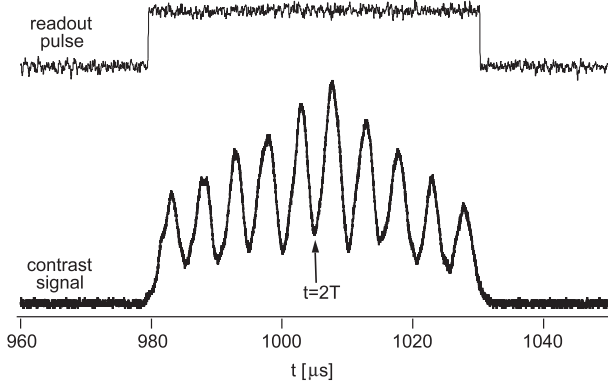


FIG. 2. Typical single shot signal from the contrast interferometer.  $T = 502.5$  s, for this example. Ten oscillations with 60% contrast and 30 s width are observed during the 50 s readout. A low-pass filter at 300 kHz (12dB per octave) was applied to the signal.

The signal also contained a small pedestal of similar width as the envelope. This consists of a constant offset from residual background light and a smoothly varying contribution from a small asymmetry between the  $j$  2hki amplitudes of  $< 5\%$ . This asymmetry creates a non-oscillating component of the 2k m after wave grating which decays with the same coherence time. The uncertainty of the fitted phase is about 10 mrad, even if we neglect the envelope function, and assume a constant amplitude extended over a few central fringes. Similar uncertainty was obtained for large times  $T = 3$  m s. We observe a shot-to-shot variation in the fitted value of the phase of about 200 mrad. We attribute this to pulse intensity fluctuations which randomly populated undesired momentum states at the  $< 10\%$  level. This resulted in spurious matter wave gratings which shifted the observed recoil phase.

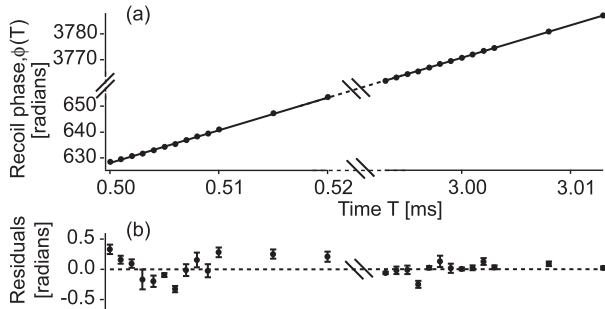


FIG. 3. Measurement of  $!_{\text{rec}}$  in sodium. Two sets of recoil phase scans, around  $T = 0.5$  m s and  $T = 3$  m s, are shown in (a). Each point is the average of five measurements. The slope of the linear fit gave  $!_{\text{rec}}$  to 7 ppm. The error bars ( $0.05 - 0.1$  rads) are shown with the fit residuals in (b).

The recoil frequency was determined by measuring the recoil phase around  $T = 0.5$  m s and around  $T = 3$  m s (Fig.3). An upper bound on  $T$  was set by the atoms falling out of the 2 m m diameter beam. A straight line fit to these data produced a value for the sodium photon recoil frequency  $!_{\text{rec},\text{Na}} = 2 - 24.9973$  kHz ( $1.6:7 \cdot 10^{-6}$ ). This is  $2 \cdot 10^{-4}$  lower than the sub-ppm value calculated using the published measurements of  $g_2, R_1, M_{\text{Na}}$  [9],  $M_e$ , and  $N_a$  [20] in Eqs.1 and 2. The systematic mean field shift due to larger population in the middle path than the extreme paths probably explains this deviation. Estimated errors from beam misalignment and wavefront curvature have the same sign as the observed deviation but several times lower magnitude.

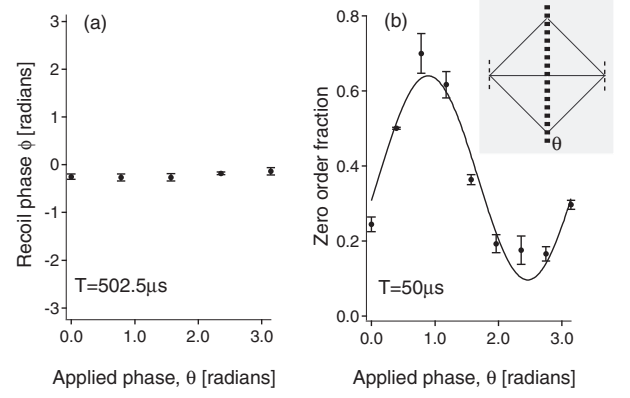


FIG. 4. Vibration insensitivity of the contrast interferometer. (a) shows the measured recoil phase at  $T = 502.5$  s from the contrast interferometer as a function of the applied phase. The recoil phase is constant and demonstrates our insensitivity to phase noise from the gratings. (b) shows the fractional population of the  $j$  hki state from the phase-sensitive interferometer (inset) for a similar scan of  $\theta$  at  $T = 50$  s. Also shown is the best-fit sinusoid of the expected period.

To demonstrate the insensitivity of the measurement to phase noise of the light due to mirror vibrations, we intentionally varied the phase of the second grating relative to the first one [21]. The contrast signal is not visibly affected by such phase variations (Fig.4 (a)). We compared this to a phase-sensitive readout method (Fig.4 (b), inset). This was realized by replacing the readout pulse with a third pulsed 1 s light grating in the Kapitza-Dirac regime, phase-locked to the first two pulses. This projected the phase of the 2k pattern at  $t = 2T$  onto the fractional populations of the states  $j$  hki,  $j$  hki, and  $j$  2hki which leave this interferometer. The populations were measured by time-of-flight absorption imaging. The  $j$  hki fraction is shown for the same variation of  $\theta$ , in Fig.4 (b). The oscillation [22] demonstrates the phase sensitivity of any position-sensitive readout.

These two interferometers respond differently to mirror vibrations. For large  $T$ , we have observed the effect of the mirror vibrations directly. At  $T = 3$  m s, the shot-to-shot fluctuations of the phase-sensitive interferometer was of

the order of the expected fringe contrast. This agrees with observations with a standard Mach-Zehnder interferometer constructed both by us and in [23]. In comparison, the stability of the contrast interferometer signal is independent of  $T$  within our measurements. This can be seen from the comparable statistical error bars for short and long times in Fig. 3 (b). In fact, the residuals and the corresponding error bars are smaller at the longer times. We attribute this to the decreased amplitude of some of the spurious gratings at longer times, due to reduced overlap of the contributing wavepackets.

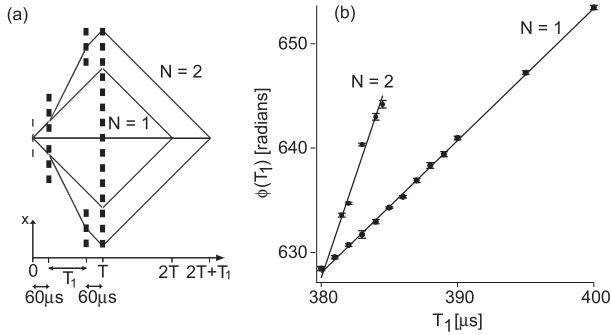


FIG. 5. Demonstration of the quadratic scaling of the recoil phase with additional photon recoils. (a) shows the  $N = 1$  (inner) and  $N = 2$  (outer) interferometers used. (b) shows the recoil phase at the recombination time under variation of  $T_1$ .

The quadratic scaling of the accumulated recoil phase with the number of transferred recoils  $N$ , was demonstrated by comparing  $N = 1$  and  $N = 2$  interferometers. An  $N = 2$  geometry, shown in Fig. 5 (a), was realized using two additional first order Bragg pulses spaced  $T_1$  apart and affecting only the extreme paths. The acceleration pulse at  $t = 60$  s drove transfers from  $|j\ 2hki\rangle$  to  $|j\ 4hki\rangle$ . The deceleration pulse at  $t = T_1 + 60$  s drove transfers from  $|j\ 4hki\rangle$  to  $|j\ 2hki\rangle$ . During the period  $T_1$ , paths 1 and 3 accumulate phase  $2^2 = 4$  times faster in the  $N = 2$  scheme than in the  $N = 1$  scheme. An additional time  $T_1$  is required for the three paths to overlap in the  $N = 2$  scheme. For this geometry, the  $N = 2$  recoil phase should therefore evolve three times faster as a function of  $T_1$  than the  $N = 1$  recoil phase. The corresponding data sets are shown in Fig. 5 (b). The linear fits give a slope ratio of  $3.06 \pm 0.1$ . At present, we do not have sufficient control over the timing and phase of the intermediate pulses to improve our  $N = 1$  measurement precision by using  $N > 1$ .

In conclusion, we have demonstrated a contrast interferometer which has several desirable features for a high precision measurement of the photon recoil frequency. Such a measurement would involve converting to an atomic fountain setup with vertical Bragg beams. In this geometry,  $T$  can be extended by nearly two orders of magnitude. Our insensitivity to phase noise from mirror vibrations should greatly alleviate vibration isolation requirements of the system for long  $T$  [13]. The order

$N$  of the interferometer must also be increased, requiring improved timing and phase control of laser pulses. Direct scaling of our current precision of  $0.01$  rads/shot, results in an estimated precision of  $< 1$  ppb/shot for  $T = 100$  ms and  $N = 20$ . A rigorous study of systematics will have to be undertaken to increase the accuracy of our measurement. Estimates show that mean field effects can be suppressed to the ppb level by reduction of atomic density to  $10^{11}$  cm $^{-3}$ , together with pulse control for  $< 5\%$  imbalance between populations in the middle and extreme paths. In addition, our methods may provide a way to study mean field effects with interferometric precision. We hope to obtain a  $< 1$  ppb value for  $\delta_{\text{rec}}$  in a second generation experiment in which BECs are created elsewhere and transported into the interferometer [24].

We thank W. Ketterle for valuable discussions. This work was supported by the NSF, ONR, ARO, NASA and the David and Lucile Packard Foundation.

- [1] R. S. Van Dyck, Jr., P. B. Schwinberg, and H. G. Dehmelt, Phys. Rev. Lett. 59, 26 (1987).
- [2] T. K. Inoshita, Phys. Rev. Lett. 75, 4728 (1995).
- [3] M. E. Cage et. al., IEEE Trans. Instr. Meas. 38, 284 (1989).
- [4] B. Taylor, Metrologia 31, 181 (1994).
- [5] C. Schwob et. al., Phys. Rev. Lett. 82, 4960 (1999).
- [6] Th. Udem et. al., Phys. Rev. Lett. 79, 2646 (1997).
- [7] T. Beier et. al., Phys. Rev. Lett. 88, 011603 (2002).
- [8] E. K. Rieger, W. Nistler, and W. Weirauch, Metrologia 35, 203 (1998).
- [9] M. P. Bradley et. al., Phys. Rev. Lett. 83, 4510 (1999).
- [10] Th. Udem et. al., Phys. Rev. Lett. 82, 3568 (1999).
- [11] 6 ppb [14]; 15 ppb (group website).
- [12] D. S. Weiss, B. C. Young, and S. Chu, Phys. Rev. Lett. 70, 2706 (1993).
- [13] B. C. Young, Ph.D. thesis, Stanford (1997).
- [14] J. M. Hensley, Ph.D. thesis, Stanford (2001).
- [15] S. B. Cahn et. al., Phys. Rev. Lett. 79, 784 (1997).
- [16] See pp. 281-282 and 379-381 in Atom Interferometry, edited by P. Bernan (Academic Press, New York, 1997).
- [17] M. Weitz, T. Heupel, and T. W. Hansch, Appl. Phys. B 65, 713 (1997).
- [18] S. Gupta et. al., C. r. Acad. Sci. IV-Phys 2, 479 (2001), and references therein.
- [19] S. Inouye et. al., Science 285, 571 (1999).
- [20] P. Juncar et. al., Metrologia 17, 77 (1981).
- [21] We scanned by electronically shifting the phase of the rf signal used to drive one of the two Bragg AOMs.
- [22] The division of population into three output ports caused 74% ( $< 100\%$ ) contrast. We have seen 100% contrast in a standard Mach-Zehnder interferometer.
- [23] Y. Torii et. al., Phys. Rev. A 61, 041602 (2000).
- [24] T. L. Gustavson et. al., Phys. Rev. Lett. 88, 020401 (2002).